STRUCTURE OPTIMIZATION TO ENHANCE ITS NATURAL FREQUENCIES BASED ON MEASURED FREQUENCY RESPONSE FUNCTIONS

YONG-HWA PARK AND YOUN-SIK PARK

Center for Noise and Vibration Control, Department of Mechanical Engineering, Korea Advanced Institute of Science and Technology, Science Town, Taejon 305-701, Korea

A measured frequency response function (FRF) based structural modification method is presented to obtain optimal structural changes to enhance its natural frequencies. Structural dynamics modification (SDM) has been widely used for improvements of built-in structures. However, the optimum design obtained by SDM differs from the true optimal solution when large modal changes happen. In this paper, a substructure-coupling concept is used to get system equations in order to extend its use to large modal changes. FRF matrix of baseline structure and those of modification structures are coupled at the connection points under the condition of force equilibrium and geometric compatibility constraints. Thus, exact modified modal properties can be calculated even for the case of large modal changes. The optimal structural modification is calculated by combining eigenvalue sensitivities and eigenvalue reanalysis technique iteratively. Special attention is given to the case where baseline structure has some unidentified structural parameters to enlighten the advantage of this proposed method. An application to the case of beam stiffener optimization indicates that the proposed method can provide an accurate optimal structural change just based on measured FRFs without any kind of numerical models.

© 2000 Academic Press

1. INTRODUCTION

Structure modification to improve its natural frequencies has received a lot of attention in wide areas since structure response is heavily influenced by its natural frequencies. To achieve effective improvement in structure natural frequencies, accurate calculations of both modified structure eigenvalues and their sensitivities subject to large modal changes are necessary. Furthermore, actual structure changes such as using beam and truss components must be practically feasible.

Numerical techniques based on FEM have been popular for this optimization purpose. However, the derived modification cannot be adopted with confidence, especially when many modelling uncertainties exist in structural parameters or in boundary conditions of complex real structures [1].

As alternatives of the numerical optimization methods, many kinds of experiment-based structural dynamics modifications (SDM) have been suggested to bypass time-consuming numerical modelling process. In many of the conventional methods, modified modal properties are predicted by utilizing some limited number of modes measured from baseline structure [2–4]. Modal perturbation [5] and linearized eigenvalue sensitivity [6] have also been used to determine structural modifications which are necessary to meet the eigenvalue requirements. But these modal domain methods are valid as long as the amount of modification is small or is just a simple rank-one modification (i.e., linear spring and point mass) [7] . The major reason for this limitation is that the accuracy of SDM is greatly dependent on the modal sufficiency of measured modes [8]. In recent years, frequency response function (FRF) based modification methods have been introduced to relieve the modal truncation problem. Wang [9] proposed a receptance formulation and extended this method to local modification. Elliot and Mitchell [10] used transfer matrix for a continuum beam modification. Chang and Park [11] suggested an FRF sensitivity formulation and applied it to a joint stiffness modification. But few structural modification methods based on FRF and modal data were introduced for realistic and thus practically applicable modifications subject to considerable eigenvalue enhancement.

Considering that modification structure is a beam and truss-type structural component, in this study, the whole system dynamic equation (baseline structure plus modifying structures) is derived using a substructure-coupling concept. The FRF matrix of baseline structure and those of modification structures are coupled at the connection points under the force equilibrium and geometric compatibility constraints. Simpson [12] developed a systematic approach to calculate exact eigenvalue solutions for substructure-coupled systems. Won and Park [13] dealt with the geometric compatibility using Lagrange multiplier to find optimal support locations to maximize its eigenvalue. Liao and Tse [14] treated the substructure coupling as a restricted eigenvalue problem. In recent years, Yee and Tsuei [15] addressed the modal force method through FRF matrix formulation. They also studied point mass and linear spring modification problem for natural frequency assignment [16]. The work in this paper endeavors to extend this substructure technique to an experimental structural optimization method. Only the measured FRF matrices of uncoupled substructures are used for optimization. Exact modified modal properties are calculated for large modal changes. Some special design variables, which are proportional to the dynamic stiffness matrices, are considered to treat realistic modifications. The eigenvalue sensitivity is formulated to find the modification direction. Finally, the optimal structural modification is calculated by combining the eigenvalue sensitivities and the exact eigenvalue reanalysis results through several iterations. To investigate the advantages of this proposed method, an experiment was performed for the beam stiffener optimization problem and the results were compared with those of the conventional modal domain modification method and FEM-based optimization results.

2. MODAL ANALYSIS FOR MODIFIED STRUCTURE

2.1. FREE VIBRATION EQUATION

A modified structure can be divided into several substructures. Thus, baseline structure and modification structures are coupled at the interface degrees of freedom as shown in Figure 1. Each single modification structure is connected to baseline structure at each interface A and C, and multiple modification structures and the baseline structure are connected to one another at interface B. For free vibrations, since there is no external force except the internal forces at the interfaces, the equation of motion of each substructure can be described in the stacked form as

$$\mathbf{H}_p(\omega)\,\mathbf{f}_p = \mathbf{x}_p, \tag{1}$$

where $\mathbf{H}_p(\omega)$ is the primitive FRF matrix containing the frequency response functions at the interfaces, $\mathbf{f}_p$ is the primitive internal force vector, and $\mathbf{x}_p$ is the primitive displacement vector defined on interface degrees of freedom. Primitive means the unassembled state. The matrix $\mathbf{H}_p(\omega)$ and the vectors $\mathbf{f}_p$, $\mathbf{x}_p$ can be written in detail as follows:

$$\mathbf{H}_p(\omega) = \begin{bmatrix} \mathbf{H}_{AA}^b(\omega) & \mathbf{H}_{AB}^b(\omega) & \mathbf{H}_{AC}^b(\omega) & \mathbf{0} & \mathbf{0} & \mathbf{0} & \mathbf{0} \\ \mathbf{H}_{BA}^b(\omega) & \mathbf{H}_{BB}^b(\omega) & \mathbf{H}_{BC}^b(\omega) & \mathbf{0} & \mathbf{0} & \mathbf{0} & \mathbf{0} \\ \mathbf{H}_{CA}^b(\omega) & \mathbf{H}_{CB}^b(\omega) & \mathbf{H}_{CC}^b(\omega) & \mathbf{0} & \mathbf{0} & \mathbf{0} & \mathbf{0} \\ \mathbf{0} & \mathbf{0} & \mathbf{0} & \mathbf{H}_{AA}^{m1}(\omega) & \mathbf{H}_{AB}^{m1}(\omega) & \mathbf{0} & \mathbf{0} \\ \mathbf{0} & \mathbf{0} & \mathbf{0} & \mathbf{H}_{BA}^{m1}(\omega) & \mathbf{H}_{BB}^{m1}(\omega) & \mathbf{0} & \mathbf{0} \\ \mathbf{0} & \mathbf{0} & \mathbf{0} & \mathbf{0} & \mathbf{0} & \mathbf{H}_{BB}^{m2}(\omega) & \mathbf{H}_{BC}^{m2}(\omega) \\ \mathbf{0} & \mathbf{0} & \mathbf{0} & \mathbf{0} & \mathbf{0} & \mathbf{H}_{CB}^{m2}(\omega) & \mathbf{H}_{CC}^{m2}(\omega) \end{bmatrix}$$

$$\tag{2a}$$

$$\mathbf{f}_p = [\mathbf{f}_A^{b^\mathrm{T}}, \mathbf{f}_B^{b^\mathrm{T}}, \mathbf{f}_C^{b^\mathrm{T}}, \mathbf{f}_A^{m1^\mathrm{T}}, \mathbf{f}_B^{m1^\mathrm{T}}, \mathbf{f}_B^{m2^\mathrm{T}}, \mathbf{f}_C^{m2^\mathrm{T}}]^\mathrm{T} \tag{2b}$$

$$\mathbf{x}_p = [\mathbf{x}_A^{b^\mathrm{T}}, \mathbf{x}_B^{b^\mathrm{T}}, \mathbf{x}_C^{b^\mathrm{T}}, \mathbf{x}_A^{m1^\mathrm{T}}, \mathbf{x}_B^{m1^\mathrm{T}}, \mathbf{x}_B^{m2^\mathrm{T}}, \mathbf{x}_C^{m2^\mathrm{T}}]^\mathrm{T}, \tag{2c}$$
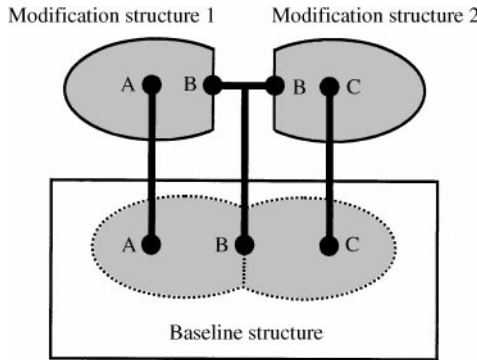

Figure 1. Structural modification by coupling of substructures and the interface degrees of freedom A, B and C.

where the superscripts $m1$, $m2$ and b denote two modification structures and baseline structure respectively and the subscripts A, B and C denote interface degrees of freedom. The displacements and the forces are subject to geometric compatibility and force equilibrium constraints at each interface as follows:

$$\mathbf{x}_A^b = \mathbf{x}_A^{m1}, \ \mathbf{x}_B^b = \mathbf{x}_B^{m1} = \mathbf{x}_B^{m2}, \ \mathbf{x}_C^b = \mathbf{x}_C^{m2}, \tag{3}$$

$$\mathbf{f}_A^b + \mathbf{f}_A^{m1} = 0, \quad \mathbf{f}_B^b + \mathbf{f}_B^{m1} + \mathbf{f}_B^{m2} = 0, \quad \mathbf{f}_C^b + \mathbf{f}_C^{m2} = 0. \tag{4}$$

Due to the constraints in equations (3) and (4), not all of the elements of $\mathbf{x}_p$ and $\mathbf{f}_p$ are independent. To form the independent vectors $\mathbf{x}_s$ and $\mathbf{f}_s$, let the elements in the primitive vectors corresponding to the modification structures be chosen as independent co-ordinates; then equations (3) and (4) can be expressed in matrix form as

$$\mathbf{U}\mathbf{x}_s = \mathbf{x}_p, \qquad \mathbf{Q}\mathbf{f}_s = \mathbf{f}_p \tag{5}$$

where the transformation matrices $\mathbf{U}$, $\mathbf{Q}$ and the independent vectors are

$$\mathbf{U} = \begin{bmatrix} I_A & 0 & 0 \\ 0 & I_B & 0 \\ 0 & 0 & I_C \\ I_A & 0 & 0 \\ 0 & I_B & 0 \\ 0 & I_B & 0 \\ 0 & 0 & I_C \end{bmatrix}, \quad \mathbf{Q} = \begin{bmatrix} -I_A & 0 & 0 & 0 \\ 0 & -I_B & -I_B & 0 \\ 0 & 0 & 0 & -I_C \\ I_A & 0 & 0 & 0 \\ 0 & I_B & 0 & 0 \\ 0 & 0 & I_B & 0 \\ 0 & 0 & 0 & I_C \end{bmatrix}, \tag{6a}$$

$$\mathbf{x}_s = [\mathbf{x}_A^{m1^T}, \ \mathbf{x}_B^{m1^T}, \ \mathbf{x}_C^{m2^T}]^T, \tag{6b}$$

$$\mathbf{f}_s = [\mathbf{f}_A^{m1^T}, \ \mathbf{f}_B^{m1^T}, \ \mathbf{f}_B^{m2^T}, \ \mathbf{f}_C^{m2^T}]^T. \tag{6c}$$

The transformation matrices $\mathbf{U}$ and $\mathbf{Q}$ generally have the relationship

$$\mathbf{Q}^T \mathbf{U} = \mathbf{0}. \tag{7}$$

Substitute equation (5) into equation (1), and pre-multiply with $\mathbf{Q}^T$ such that

$$\mathbf{Q}^T \mathbf{H}_p(\omega) \mathbf{Q}\mathbf{f}_s = \mathbf{Q}^T \mathbf{U}\mathbf{x}_s = \mathbf{0}. \tag{8}$$

Then we have the free vibration equation of modified structure for independent force vector

$$\mathbf{H}(\omega)\mathbf{f} = \mathbf{0}, \tag{9}$$

where $\mathbf{f} = \mathbf{f}_s$ and

$$\mathbf{H}(\omega) = \mathbf{Q}^T \mathbf{H}_p(\omega) \mathbf{Q} = \left(\begin{bmatrix} \mathbf{H}_{AA}^b(\omega) & \mathbf{H}_{AB}^b(\omega) & \mathbf{H}_{AB}^b(\omega) & \mathbf{H}_{AC}^b(\omega) \\ \mathbf{H}_{BA}^b(\omega) & \mathbf{H}_{BB}^b(\omega) & \mathbf{H}_{BB}^b(\omega) & \mathbf{H}_{BC}^b(\omega) \\ \mathbf{H}_{BA}^b(\omega) & \mathbf{H}_{BB}^b(\omega) & \mathbf{H}_{BB}^b(\omega) & \mathbf{H}_{BC}^b(\omega) \\ \mathbf{H}_{CA}^b(\omega) & \mathbf{H}_{CB}^b(\omega) & \mathbf{H}_{CB}^b(\omega) & \mathbf{H}_{CC}^b(\omega) \end{bmatrix} \right.$$

$$+ \begin{bmatrix} \mathbf{H}_{AA}^{m1}(\omega) & \mathbf{H}_{AB}^{m1}(\omega) & \mathbf{0} & \mathbf{0} \\ \mathbf{H}_{BA}^{m1}(\omega) & \mathbf{H}_{BB}^{m1}(\omega) & \mathbf{0} & \mathbf{0} \\ \mathbf{0} & \mathbf{0} & \mathbf{H}_{BB}^{m2}(\omega) & \mathbf{H}_{BC}^{m2}(\omega) \\ \mathbf{0} & \mathbf{0} & \mathbf{H}_{CB}^{m2}(\omega) & \mathbf{H}_{CC}^{m2}(\omega) \end{bmatrix} \Bigg)$$

$$= (\mathbf{H}^b(\omega) + \mathbf{H}^m(\omega)). \tag{10}$$

Equation (9) is called the modal force equation, which is the key equation in this study. The modal force vector $\mathbf{f}$ consists of the internal forces acting on the modification substructures. The modal force matrix, $\mathbf{H}(\omega)$, is the summation of FRF matrix of the baseline structure, $\mathbf{H}^b(\omega)$, and that of the modification substructure, $\mathbf{H}^m(\omega)$. Experimentally measured FRFs can be used directly to form the modal force equation bypassing the numerical modelling process as shown in equation (10). For a general modification case in which N modification structures are involved, the modal force equations can be constructed by coupling each FRF matrix of substructure through the transformation matrix $\mathbf{Q}$ in a similar way. If there is no interface degree of freedom outside the baseline structure, the result is expressed in the general form as

$$\mathbf{H}(\omega)\mathbf{f} = [\mathbf{H}^b(\omega) + diag\,(\mathbf{H}^{m1}(\omega), \mathbf{H}^{m2}(\omega), \ldots, \mathbf{H}^{mN}(\omega))]\,\mathbf{f} = \mathbf{0}, \tag{11}$$

where $diag(\bullet)$ represents the block diagonal matrix containing FRF matrices in the main diagonal. The modal force vector $\mathbf{f}$ is defined as

$$\mathbf{f} = [\mathbf{f}^{m1^{\mathrm{T}}}, \ \mathbf{f}^{m2^{\mathrm{T}}}, \ldots, \mathbf{f}^{mN^{\mathrm{T}}}]^{\mathrm{T}}. \tag{12}$$

$\mathbf{H}^{mi}(\omega)$ (for $j = 1, 2, \ldots, N$) is the FRF matrix of the jth modification structure. The element of $\mathbf{H}^b(\omega)$, i.e., $h_{ij}^b(\omega)$, is the FRF of the baseline structure between the interface co-ordinates corresponding to ith and jth modal forces contained in the modal force vector $\mathbf{f}$.

2.2. MODIFIED MODAL PROPERTIES

Natural frequencies and modal forces are the solutions of modal force equation, i.e., equation (11). From the condition that equation (11) has non-trivial solution $\mathbf{f}$, the determinant of equation (11) must be equal to zero. Hence, we have characteristic equations such as

$$\mathrm{Det}\,(\mathbf{H}(\omega)) = 0. \tag{13}$$

Since $\mathbf{H}(\omega)$ is a rational function of frequency ω, the determinant search method is commonly used to find the roots of the above characteristic equation. Simpson [12] used the Newton–Raphson method and Liao and Tse [14] suggested a spectrum-slicing formulation. Yee and Tsuei [15] suggested an improved characteristic equation

$$\mathrm{Det}\,(\mathbf{H}(\omega)) \prod_{k=1}^{N_s} \prod_{j=1}^{S_k} (\omega_j^{(k)^2} - \omega^2) = 0, \tag{14}$$

where $\omega_j^{(k)}$ is the jth natural frequency of the kth substructure, N_s is the number of substructures and S_k is the number of modes of the kth substructure in the frequency range of interest. Equation (14) can avoid the numerical instabilities which arise in the vicinities of the natural frequencies of uncoupled substructures when the determinants are calculated from the measured FRFs. For this reason, the stabilized equation (14) is used for calculation of determinants in this work. Natural frequencies are obtained using the bisection method. Then the modal force vector $\mathbf{f}$ is calculated by solving the rank-deficient modal force equation, i.e., equation (11), for the identified natural frequency.

Under the assumption that the measurements are free of noise, the results of eigenvalue analysis are exact for both small and large amounts of modifications since there is no approximation in the eigenvalue solution procedure. Furthermore, since the order of modal force matrix is the number of connection degrees of freedom, large computing efforts for solving the eigenvalue problem of an entire structure can be avoided.

2.3. PRACTICAL MODIFICATIONS

In order to perform the eigenvalue reanalysis, the modal force matrices after successive modifications should be obtained by updating the FRF matrix of modified part in equation (11) as

$$\mathbf{H}(\omega, d) = [\mathbf{H}^b(\omega) + \mathbf{H}^m(\omega, d)], \tag{15}$$

where d denotes a design variable. Then the new modal properties can be reanalyzed from the determinant search of $\mathbf{H}(\omega, d)$.

To have practical structural changes such as beam and truss modifications, a special design variable which is proportional to the structural element matrix, which is called design proportional element, is used. The design proportional elements have been widely used for reanalysis [4] and model-updating purpose [17]. Some of the commonly used structural elements listed in Table 1 show the characteristics of design proportional element; stiffness, mass and damping matrices of the structure are proportional to the design variable d as follows:

$$\mathbf{K}^m(d) = d\mathbf{K}_0^m, \quad \mathbf{M}^m(d) = d\mathbf{M}_0^m, \quad \mathbf{C}^m(d) = d\mathbf{C}_0^m = d(\alpha \mathbf{M}_0^m + \beta \mathbf{K}_0^m), \tag{16}$$

where proportional damping is assumed. In this case, the design variable can be factored out from the system matrices, and so the calculations of element matrices become simple. For these elements, the dynamic stiffness matrix of the modification structure, $\mathbf{D}^m(\omega, d)$, becomes

$$\mathbf{D}^m(\omega, d) = \mathbf{K}^m(d) + i\omega\mathbf{C}^m(d) - \omega^2 \mathbf{M}^m(d) = d\mathbf{D}_0^m(\omega), \tag{17}$$

where $\mathbf{D}_0^m(\omega) = \mathbf{K}_0^m + i\omega\mathbf{C}_0^m - \omega^2 \mathbf{M}_0^m$. Hence the frequency response matrix, $\mathbf{H}^m(\omega, d)$, can be written as

$$\mathbf{H}^m(\omega, d) = [\mathbf{D}^m(\omega, d)]^{-1} = [d\mathbf{D}_0^m(\omega)]^{-1} = \frac{1}{d} \mathbf{H}_0^m(\omega). \tag{18}$$

The FRF matrix of modification structure, $\mathbf{H}^m(\omega, d)$, is proportional to the reciprocal of design variable. $\mathbf{H}_0^m(\omega)$ is called frequency response element in this study, which is the inversion of the dynamic stiffness matrix of modification structure, $\mathbf{D}_0^m(\omega)$. The frequency response element is obtained from *a priori* measurements of the FRF matrix $\mathbf{H}^m(\omega, d_a)$ by using equation (18) as follows:

$$\mathbf{H}_0^m(\omega) = d_a \mathbf{H}^m(\omega, d_a), \tag{19}$$

where d_a is an arbitrarily chosen design variable. Using the frequency response element, the modal force matrix in equation (15) can be formulated with respect to design variable d and frequency response elements such as

$$\mathbf{H}(\omega, d) = \left[\mathbf{H}^b(\omega) + \frac{1}{d}\,\mathbf{H}_0^m(\omega)\right]. \tag{20}$$

When N design proportional elements are involved, the modal force equation for N design variables can be written from equations (11) and (18) as

$$\mathbf{H}(\omega, \mathbf{d})\mathbf{f} = \left[\mathbf{H}^b(\omega) + diag\left(\frac{1}{d_1}\,\mathbf{H}_0^{m1}(\omega), \frac{1}{d_2}\,\mathbf{H}_0^{m2}(\omega), \dots, \frac{1}{d_N}\,\mathbf{H}_0^{mN}(\omega)\right)\right]\mathbf{f} = \mathbf{0}, \tag{21}$$
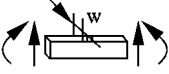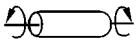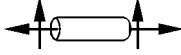
where the design vector $\mathbf{d}$ denotes $[d_1, d_2, \dots, d_N]^T$ and $\mathbf{H}_0^{mj}(\omega)$ (for $j = 1, 2, \dots, N$), is the frequency response element for the jth modification structure. The actual structure changes such as beam stiffener, torsion shaft and truss members listed in Table 1 can be treated with equation (21). Note that the modal force equation can be obtained by just simply updating the design vector $\mathbf{d}$ without any further measurements of FRF matrices for the modification structures as well as for the baseline structure during the successive design modifications.

3. EIGENVALUE SENSITIVITY ANALYSIS

Design modification directions are obtained by examining eigenvalue sensitivities with respect to design changes. Simpson [12] formulated the

TABLE 1

Common structural elements and proportional design variables

	Element	Design variable
	Point mass	Mass
	Linear/torsional spring	Stiffness
	Bending beam	Width
	(rectangular cross-section)	
	Torsional shaft	Polar moment of
	(circular cross-section)	cross-sectional area
	Truss and rod	Cross-sectional area
	(arbitrary cross-section)	

eigenvalue sensitivity equation for a coupled system using derivatives of mass and stiffness matrices with respect to design variables. In this work, the eigenvalue sensitivity will be formulated with the modal force equation, i.e., equation (21) by directly differentiating the FRF matrices with design variables.

For natural frequency ω_n and modal force vector $\mathbf{f}$ of current design vector $\mathbf{d}$, differentiation of equation (21) with respect to design variable d_j yields

$$\frac{\mathrm{d}}{\mathrm{d}d_j}(\mathbf{H}(\omega_n, \mathbf{d})\mathbf{f}) = \frac{\mathrm{d}\mathbf{H}(\omega_n, \mathbf{d})}{\mathrm{d}d_j}\mathbf{f} + \mathbf{H}(\omega_n, \mathbf{d})\frac{\mathrm{d}\mathbf{f}}{\mathrm{d}d_j}$$

$$= \frac{\partial\mathbf{H}(\omega_n, \mathbf{d})}{\partial\omega_n}\frac{\mathrm{d}\omega_n}{\mathrm{d}d_j}\mathbf{f} + \frac{\partial\mathbf{H}(\omega_n, \mathbf{d})}{\partial d_j}\mathbf{f} + \mathbf{H}(\omega_n, \mathbf{d})\frac{\mathrm{d}\mathbf{f}}{\mathrm{d}d_j}$$

$$= 0 \quad \text{for } j = 1, 2, \ldots, N. \tag{22}$$

Pre-multiply equation (22) by $\mathbf{f}^{\mathrm{T}}$ such that

$$\mathbf{f}^{\mathrm{T}}\frac{\partial\mathbf{H}(\omega_n, \mathbf{d})}{\partial\omega_n}\frac{\mathrm{d}\omega_n}{\mathrm{d}d_j}\mathbf{f} + \mathbf{f}^{\mathrm{T}}\frac{\partial\mathbf{H}(\omega_n, \mathbf{d})}{\partial d_j}\mathbf{f} + \mathbf{f}^{\mathrm{T}}\mathbf{H}(\omega_n, \mathbf{d})\frac{\mathrm{d}\mathbf{f}}{\mathrm{d}d_j} = 0. \tag{23}$$

From equation (21), the last term on the left-hand side of equation (23) vanishes since $\mathbf{H}(\omega_n, \mathbf{d})$ is symmetric. For normalized modal force vector $\mathbf{f}$ such that

$$\mathbf{f}^{\mathrm{T}}\frac{\partial\mathbf{H}(\omega_n, \mathbf{d})}{\partial\omega_n}\mathbf{f} = 1, \tag{24}$$

the eigenvalue sensitivity is obtained as

$$\frac{\mathrm{d}\omega_n}{\mathrm{d}d_j} = -\mathbf{f}^{\mathrm{T}}\frac{\partial\mathbf{H}(\omega_n, \mathbf{d})}{\partial d_j}\mathbf{f}. \tag{25}$$

Hence, we have the eigenvalue sensitivity equation by directly differentiating the modal force matrix, $\mathbf{H}(\omega_n, \mathbf{d})$, in equation (21) with respect to design variables as follows:

$$\frac{\mathrm{d}\omega_n}{\mathrm{d}d_j} = \frac{1}{d_j^2}\mathbf{f}^{mj^{\mathrm{T}}}\mathbf{H}_0^{mj}(\omega_n)\mathbf{f}^{mj} \quad \text{for } j = 1, 2, \ldots, N, \tag{26}$$

where $\mathbf{f}^{mj}$ is the modal force vector corresponding to the jth modification structure. In equation (26), complex derivative terms are not included but the explicit form of the derivative of FRF matrix is shown in a simple manner due to the proportionality of design variable. Note that equation (26) is formulated based on an identified force state and response model which can be directly measured from the structure. The eigenvalue sensitivity vector for current design vector $\mathbf{d}$ is defined from equation (26) as

$$\mathbf{s} \equiv \left[\frac{\mathrm{d}\omega_n}{\mathrm{d}d_1}, \frac{\mathrm{d}\omega_n}{\mathrm{d}d_2}, \ldots, \frac{\mathrm{d}\omega_n}{\mathrm{d}d_N}\right]^{\mathrm{T}}. \tag{27}$$

This vector will be used in optimization to find the modification directions for natural frequency improvement.

4. OPTIMIZATION PROCEDURE

In this work, raising the eigenvalue is the object of design optimization. The eigenvalue sensitivity vector defined in equation (27) shows the steepest direction to raise the eigenvalue. Thus, it will provide a suboptimal structural change from the current design. Because of the non-linear nature of eigenvalues with design change, the optimal set of design variables will be obtained through iterations. Iteration procedure means successive design modifications and it needs eigenvalue sensitivities and eigenvalue solving techniques as mentioned in the preceding section. No further FRF acquisition is needed but just initial FRFs obtained from both baseline structure and modification structures are enough for this design optimization. In the modification stage, extra constraints on the design variables can be considered. The optimization procedure can be summarized in four steps as follows. (i) *FRF measurements*: FRFs of baseline structure and frequency response elements are measured as equation (19). Set initial design vector **d**. (ii) *Modal analysis*: modal force equation is constructed for current design vector **d** by using equation (21). Natural frequency and modal force vector are identified by determinant search of characteristic equation shown in equation (14). (iii) *Design modification*: eigenvalue sensitivity vector **s** for the current design is calculated from the identified modal properties by using equations (26) and (27). Design vector **d** is modified based on the eigenvalue sensitivity vector **s** subject to extra constraints on design variables. (iv) *Optimality check*: check the optimality criterion and if it is not satisfied, continue the procedure from step (ii) until the optimal solutions is obtained.

5. APPLICATION OF BEAM STIFFENER OPTIMIZATION

Experimental structural optimization with bending beam stiffeners was performed to demonstrate the effectiveness of the proposed method. The baseline structure is a steel square plate having dimensions 800 mm × 800 mm × 3 mm as shown in Figure 2(a). The plate is simply supported at each corner. Figure 2(b) shows the first mode calculated from FE model of the plate, which has a modulus of elasticity of 200 GPa, and a density of 7800 kg/m^3. In an actual structure, there may be some modelling uncertainties in material properties and/or in boundary conditions. Especially, modal properties of a system are very sensitive to its boundary conditions in many cases. In order to investigate the effects of modelling uncertainties on optimization results, boundary condition was given imperfectly such that a linear spring having "unknown" value of stiffness was placed at the lower-left corner of the plate. Figure 2(c) shows the implemented (imperfectly supported) plate in the experiment and Figure 2(d) shows its measured first mode.

5.1. SINGLE-BEAM MODIFICATION

To verify the accuracy of calculated natural frequencies, a steel beam stiffener was attached to the baseline plate and then modified natural frequencies were measured. Then the measured natural frequencies were directly compared with the
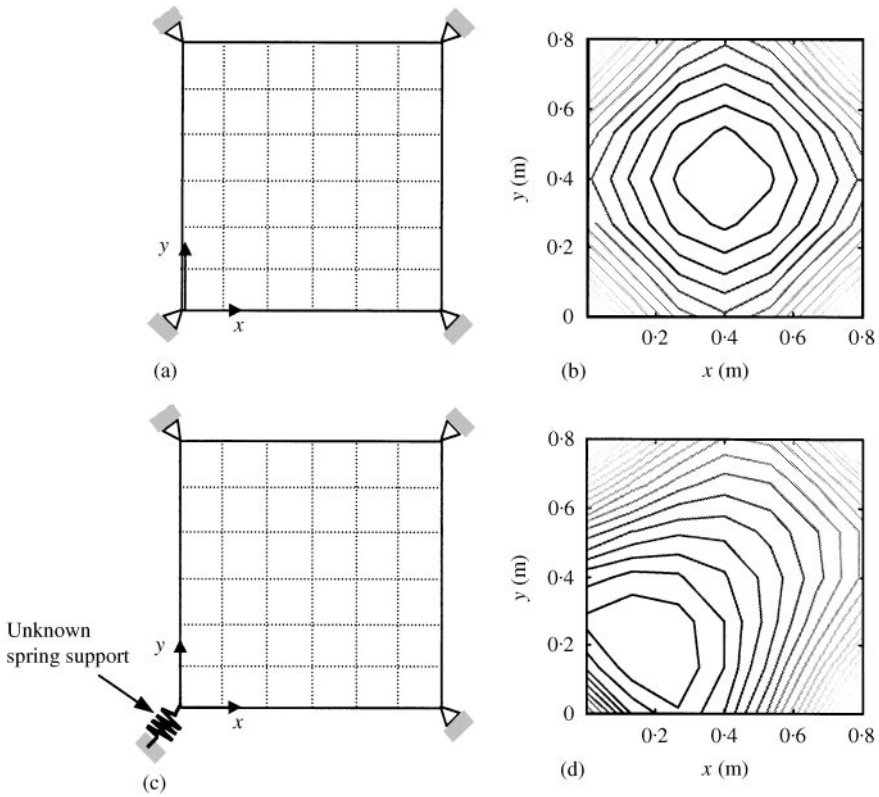
Figure 2. Baseline structure: (a) ideal simply supported plate; (b) calculated first mode of the ideal plate ($\omega_1 = 8\cdot10$ Hz); (c) implemented plate having unknown spring support; (d) measured first mode of the implemented plate ($\omega_1 = 7\cdot81$ Hz).

calculated natural frequencies from the proposed method. A rectangular cross-sectional beam having a length of 533 mm, height of 8·5 mm and width of 25 mm was attached to the plate of five nodes as shown in Figure 3. The beam stiffener is modelled with a combination of four frequency response elements as shown in Figure 3. From equation (21), the modal force equation in this case is formulated as

$$\left[\mathbf{H}^b(\omega) + diag\left(\frac{1}{d_1} \mathbf{H}_0^{m1}(\omega), \frac{1}{d_2} \mathbf{H}_0^{m2}(\omega), \frac{1}{d_3} \mathbf{H}_0^{m3}(\omega), \frac{1}{d_4} \mathbf{H}_0^{m4}(\omega) \right) \right] \mathbf{f} = \mathbf{0}, \quad (28)$$

where $\mathbf{f} = [\mathbf{f}_1^T, \mathbf{f}_2^T, \mathbf{f}_3^T, \mathbf{f}_4^T]^T$ and $\mathbf{f}_j$ (4 × 1) are the internal force vectors (vertical forces and angular moments at each of the two attachment nodes) exerted on the jth bending beam element and the design variables, d_j (j = 1,2,3,4) are the widths of elements, 25 mm in this case. The experiment set-up is shown in Figure 4. A frequency band including seven natural modes of the plate was chosen. The point and transfer FRFs of the baseline plate where measured at five attachment nodes to construct $\mathbf{H}^b(\omega)$. Figure 5 shows measured FRFs. Since all of the beam segments have equal lengths, heights and the same material properties in this case, the
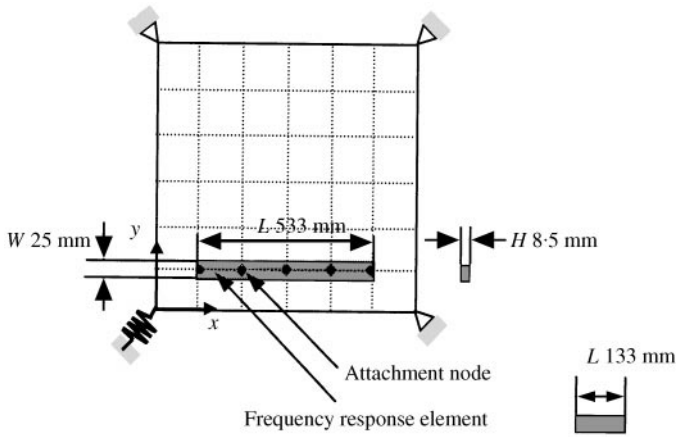
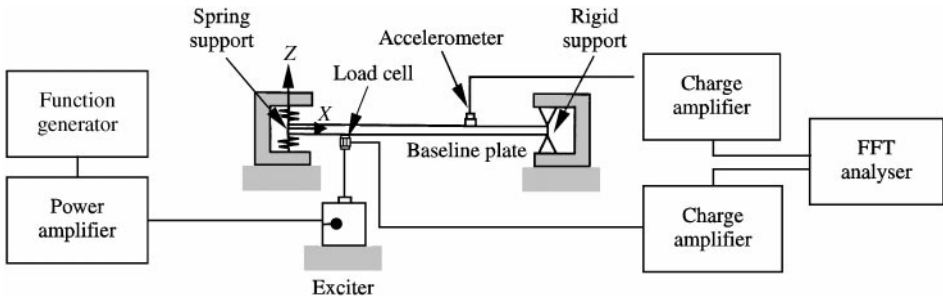Figure 3. Single-beam modification and modelling by frequency response elements.

Figure 4. Schematic diagram of experiment set-up for FRF measurement (side view of the plate at $y = 0$).
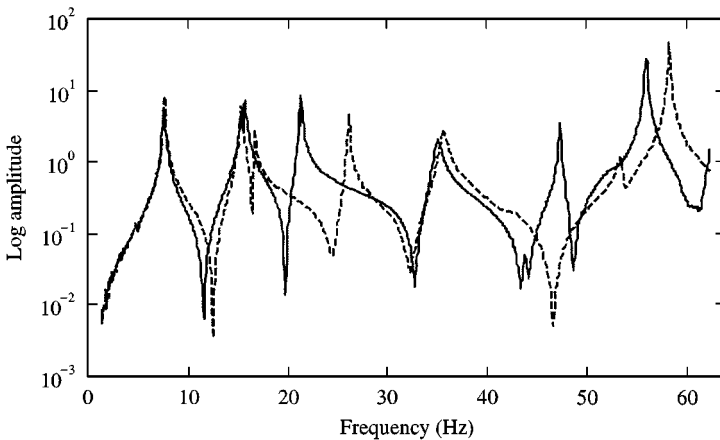

Figure 5. FRF measurements of plate. ——, point FRF of baseline plate; - - - -, point FRF of beam-modified plate.

frequency response elements are identical,

$$\mathbf{H}_0^{m1}(\omega) = \mathbf{H}_0^{m2}(\omega) = \mathbf{H}_0^{m3}(\omega) = \mathbf{H}_0^{m4}(\omega) = \mathbf{H}_0^{m}(\omega). \tag{29}$$

The frequency response element, $\mathbf{H}_0^{m}(\omega)$, was measured from a steel beam having a length of 133 mm, height of 8·5 mm and width of 8·5 mm with free–free boundary condition. Figure 6 shows the measured FRF and the calculated FRF of the frequency response element from equation (19). In this case, d_a is 8·5 mm. The rotational deflections in the FRF matrices of the plate and the beam elements were not measured directly but calculated from the derivatives of the third order polynomial which fits the adjacent translational deflections [18].

Natural frequencies of the modified system are obtained by determinant search from the formulated modal force matrix in equation (28). The determinant search results are shown in Figure 7. The roots of the determinant indicate modified natural frequencies. The measurements and calculations of natural frequencies are listed in Table 2. The eigenvalue analysis results from the proposed method are accurate to the measured values within 4% error.

The results were also compared with those from the conventional modal synthesis method [3–5]. Seven identified modes in the frequency band of interest were used for the modal synthesis method. Table 2 shows that the higher modes show larger errors, which have been observed in many cases. These errors are mostly attributed to modal truncations. However, the proposed method predicts the modified natural frequencies to be considerably accurate even for higher modes. That is because the measured FRFs include the full information of residual modes. Furthermore, the proposed method can estimate a large natural frequency change fairly accurately. In this beam-stiffened plate case, the fourth natural frequency was raised by 21·4% (from 21·56 to 27·17 Hz) by beam modification. But as shown in Table 2, the large eigenvalue change can be predicted successfully in the proposed method with only 2·9% error. On the other hand, the modal synthesis method can predict this mode with 10·6% error.
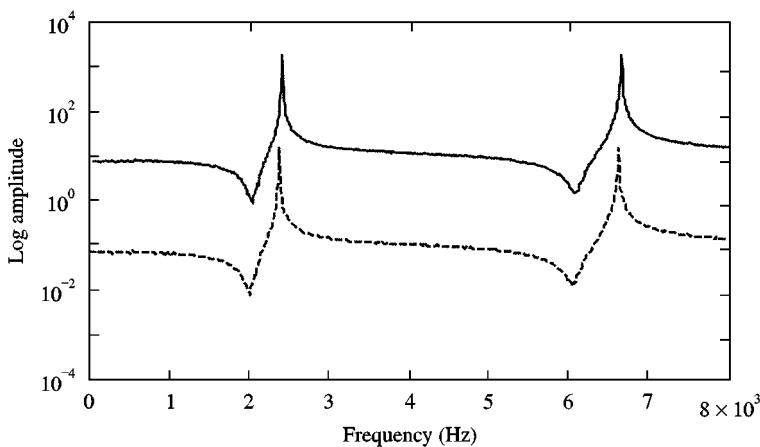

Figure 6. FRF of beam element ———, measured point FRF of beam with free-free boundary condition; - - - -, calculated FRF of frequency response element from equation (19).
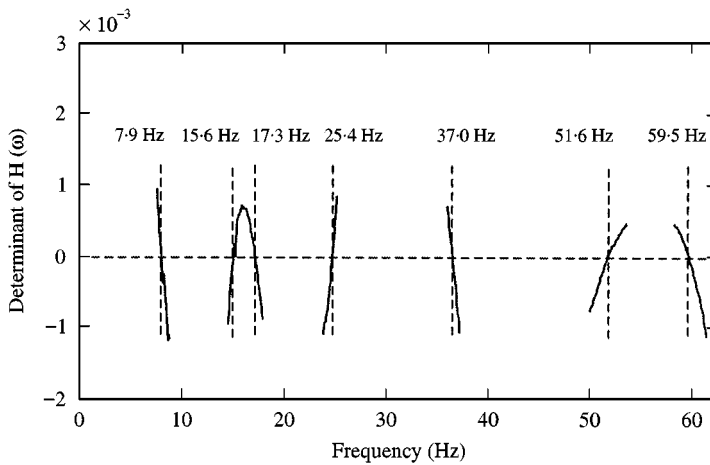
Figure 7. Determinant curve of modified plate and identified natural frequencies.

TABLE 2

Measured and calculated natural frequencies of modified plate

Mode no.	Measurement		Proposed method		Modal synthesis method	
	Baseline	Modified	Natural frequency	Error (%)[†]	Natural frequency	Error (%)[†]
1	7·81	7·81	7·89	1·02	7·98	2·18
2	15·71	15·39	15·63	1·56	15·59	1·30
3	15·78	16·72	17·34	3·71	17·27	3·29
4	21·56	26·17	25·40	2·94	28·95	10·62
5	35·16	35·70	36·95	3·50	38·90	8·96
6	47·34	53·44	51·56	3·52	72·31	35·31
7	56·25	58·36	59·45	1·87	89·23	52·90

[†] The errors are relative differences between the calculated natural frequencies and the measured modified natural frequencies.

5.2. DISTRIBUTED BEAM MODIFICATION

The single-beam modification procedure can be easily extended to multi-beam stiffening cases using the same sort of equation, i.e., equation (28). In this section, an optimization problem to get beam stiffener design to maximize fundamental natural frequency will be dealt with. The problem is how to distribute the beam stiffener on the baseline plate structure to raise the eigenvalue. Figure 8 shows the layout of beam stiffeners for this optimization. Forty equally distributed beam elements are attached at 25 nodes of the plate. The object is to maximize the fundamental natural frequency of the beam-stiffened plate by changing the widths of the beam elements. The design variables are the widths d_j ($j = 1, 2, \ldots, 40$) of
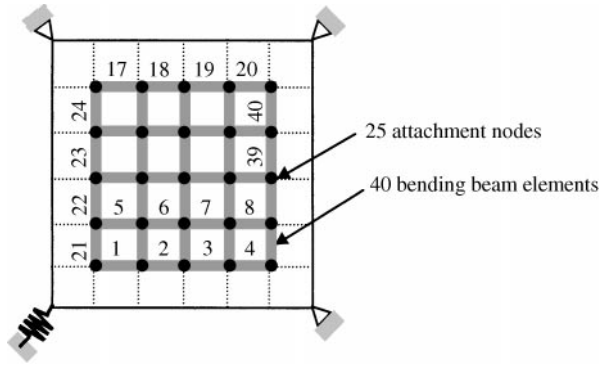
Figure 8. Layout of beam elements for optimization.

beam elements in this case and the design vector can be written as

$$\mathbf{d} = [d_1, d_2, \ldots, d_{40}]^{\mathrm{T}}. \tag{30}$$

The optimization problem can be defined mathematically as follows:

$$\text{maximize} \quad \omega_1(\mathbf{d}) \tag{31}$$

$$\text{subject to} \quad \sum_{j=1}^{40} m_j = \sum_{j=1}^{40} (\rho_j L_j H_j) d_j \leqslant M_{max}, \tag{32}$$

$$0 \leqslant d_j \leqslant d_{max}, \quad \text{for } j = 1, 2, \ldots, 40 \tag{33}$$

where m_j, ρ_j, L_j and H_j are the mass, density, length and height of the jth beam element. The total amount of beam modification is limited to M_{max} (2·0 kg), which is a 13·2% increase from the mass of the baseline plate (15·1 kg). The design variables are also restricted by the upper bound of the beam width, d_{max} (30 mm). Each rectangular cross-sectional beam element has the same length, height and material properties. The same frequency response element, $\mathbf{H}_0^m(\omega)$ (4 × 4; two translational deflections and two rotational deflections) in the previous single-beam modification case is used to model the distributed beam elements. The modal force equation in this case can be written from equation (21) as

$$\left[\mathbf{H}^b(\omega) + diag\left(\frac{1}{d_1} \mathbf{H}_0^m(\omega), \frac{1}{d_2} \mathbf{H}_0^m(\omega), \ldots, \frac{1}{d_{40}} \mathbf{H}_0^m(\omega) \right) \right] \mathbf{f} = \mathbf{0}. \tag{34}$$

The point and transfer FRFs of the baseline plate were measured at 25 attachment nodes to construct $\mathbf{H}^b(\omega)$. The rotational deflections in $\mathbf{H}^b(\omega)$ were obtained from the fitting polynomials of adjacent translational deflections [18].

Based on the modal force equation shown in equation (34) and the eigenvalue sensitivities obtained from equation (26), the optimization was performed through iterations. The initial widths were selected to be 2·5 mm for all the beam elements. The gradient projection method of Rosen [19] was used to solve this linear constrained optimization problem. For the convergence criterion, the Karush–Kuhn–Tucker condition is checked at each iteration step. Figure 9 shows the variations of eigenvalue sensitivities of certain beam elements during the
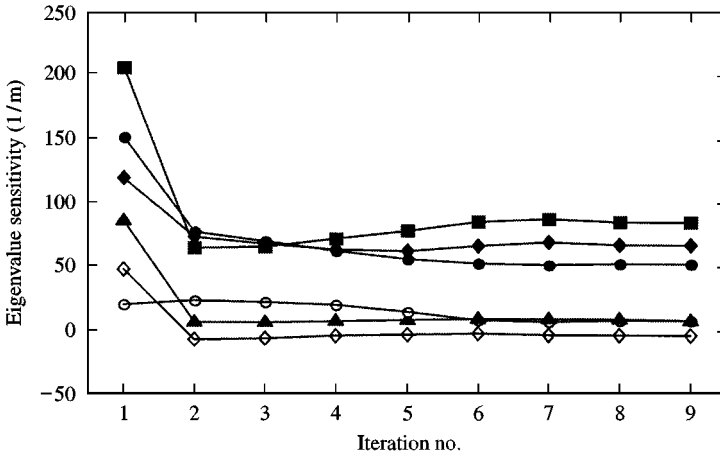
Figure 9. Variations of eigenvalue sensitivities with respect to beam widths versus iterations: ▲, element 3; ◇, 8; ●, 17; ○, 19; ■, 24; ◆, 40.
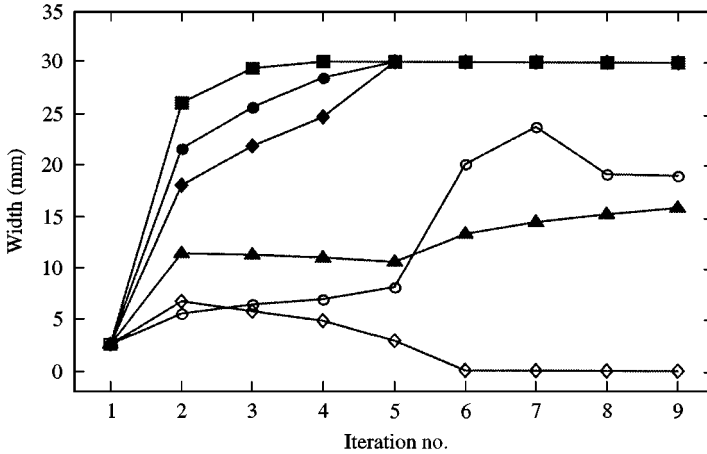

Figure 10. Variations of beam widths versus iterations: ▲, element 3; ◇, 8; ●, 17; ○, 19; ■, 24; ◆, 40.

iterations. Based on the sensitivities and the design variable constraints in equations (32) and (33), the widths are modified and its modal properties are reanalyzed from the updated equation (34) at the next iteration step. Figure 10 shows the variation of widths of certain elements during the optimization process. Figure 11 shows the change of modified natural frequency. Optimal fundamental natural frequency was found to be 10·32 Hz, which is 32% higher than the natural frequency of the baseline plate, 7·81 Hz. The maximum-stiffened beam widths are plotted in Figure 13(a). The distribution is not symmetric because the lower-left corner of the plate is spring supported.

In order to investigate the advantages of the proposed method, the optimization result was compared with those from the modal perturbation method and
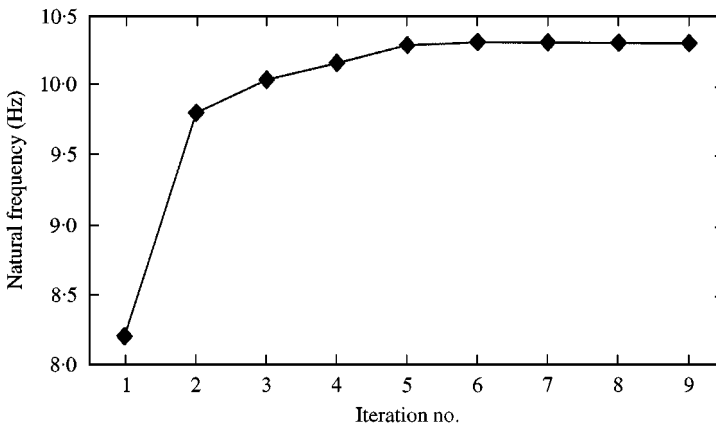
Figure 11. Change of fundamental natural frequency versus iterations.

FE-analysis-based optimization. For the comparison, the same optimization problem defined in equations (30)–(33) was solved independently using each method. The modal perturbation method has been commonly used for determining the structural modification based on the measured modal properties of the baseline structure. To calculate the perturbation-based optimal beam modification, the first order eigenvalue perturbation of the foundamental natural frequency was calculated as follows [5]:

$$\Delta\omega_1^{mj^2} = \phi_1^{\mathrm{T}} \left(\Delta\mathbf{K}^{mj} - \omega_1^2 \Delta\mathbf{M}^{mj} \right) \phi_1 \quad \text{for } j = 1, 2, \ldots, 40, \tag{35}$$

where $\Delta\omega_1^{mj^2}$ is the eigenvalue perturbation of the first mode due to stiffness and mass perturbations of the jth beam element. ω_1 and ϕ_1 are natural frequency and mode shape of the measured first mode of the baseline plate shown in Figure 2(d). The perturbation matrices, $\Delta\mathbf{K}^{mj}$ and $\Delta\mathbf{M}^{mj}$ ($j = 1, 2, \ldots, 40$), were obtained from the FE models of the beam elements in Figure 8 having the initial width of 2·5 mm. Figure 12 shows the calculated eigenvalue changes due to perturbation of each beam element. The width modifications were obtained in one step by using these sensitivities and the same design variable constraints in equations (32) and (33). Figure 13(b) shows the resulting distribution of the beam widths over the plate.

   Also the FE-analysis-based optimization was performed. In the procedure, two different FE models of the baseline plate were used. One is the "ideal" plate model shown in Figure 2(a) and the other is the "adjusted" plate model which is supported by a spring support having stiffness 27 kN/m instead of simple support at the lower-left corner. The fundamental natural frequency of the adjusted plate model is 7·83 Hz, which is fairly close to the measured natural frequency, 7·81 Hz. The optimization code was written in MATLAB Structural Dynamics Toolbox and the gradient projection method of Rosen was used for non-linear optimization programming. Iterative calculations of eigenvalue analysis and its sensitivity analysis were performed to solve the standard optimization problem defined in equations (31)–(33). The optimization result of the beam widths is shown in Figures 13(c) and 13(d).
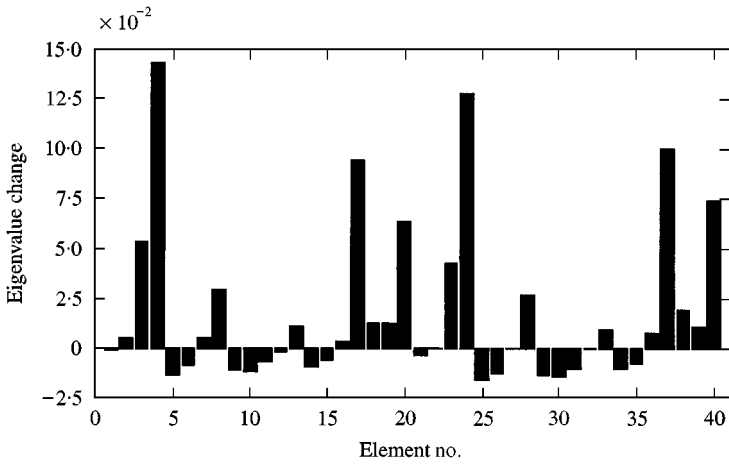
Figure 12. First order eigenvalue perturbations due to perturbation of each beam element.
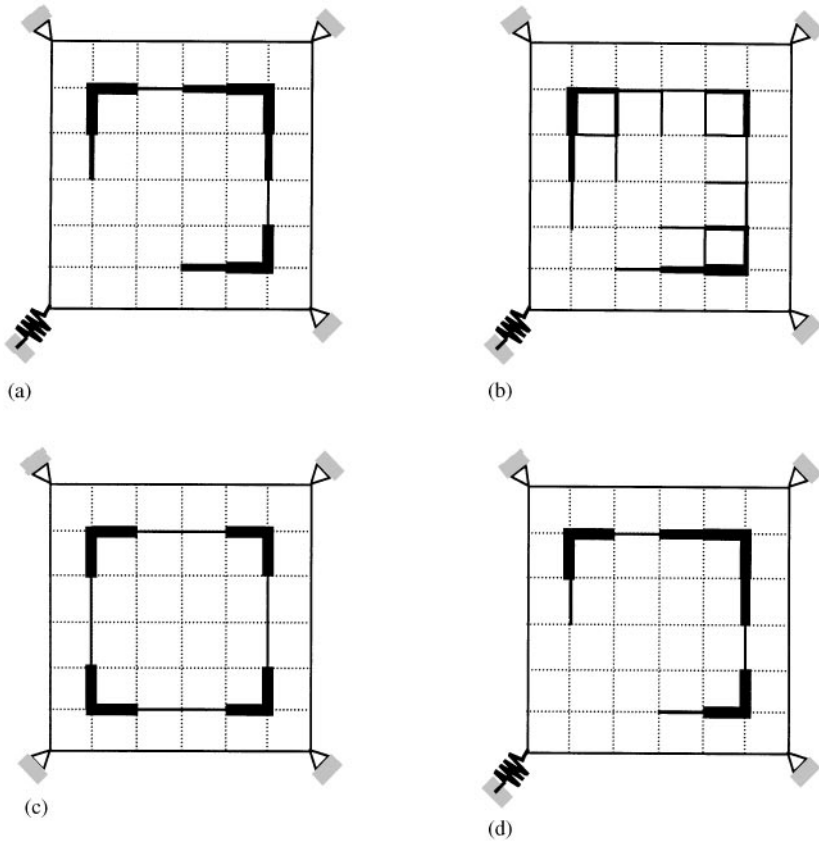

Figure 13. Distributions of optimized beam elements from three different modification methods: (a) proposed method; (b) perturbation method; (c) FEM using ideal plate model (four simple supports); (d) FEM using adjusted plate model (three simple supports and a spring support having stiffness 27 kN/m).

TABLE 3

Optimized natural frequencies from the three different optimization methods

	Baseline	Optimized			
		Proposed method	Perturbation method	FEM with ideal model	FEM with adjusted model
Natural frequency (Hz)	7·81	10·32	9·93	10·05	10·31
Improvement (%)[†]	—	32·1	27·1	28·6	32·1

[†] The improvements are relative increments from the baseline natural frequency to the optimized natural frequencies.

To compare the optimization performances, maximized fundamental natural frequencies of the three methods were calculated by using the verified modal force equation, i.e., equation (34) for different optimized sets of widths. Table 3 shows the resulting natural frequencies and its improvements. The results indicate that the proposed method provides optimal results superior to other methods except FEM with an adjusted plate model in this beam-modification problem.

Both the perturbation and the proposed method have the advantage that the optimal structural modifications can be found just from measured dynamic characteristics of baseline structures. But the perturbation-based modification shown in Figure 13(b), which has a more scattered pattern compared with that of the proposed method, is not a true optimal solution but an approximate one since it uses linearized perturbation of the natural frequency. On the other hand, the non-linear nature of the eigenvalue change due to structural modification is considered accurately in this proposed method. In other words, the sub-optimal structural change determined by the eigenvalue sensitivity, which varies in a non-linear fashion according to the accumulated structural changes, can be traced accurately through the successive modifications. This comes from the fact that the modal changes can be found accurately even for large modal changes since the equation of motion of the proposed methods is based on FRF, including the information of full modes. As shown in Figure 9, the sensitivities vary as iterations are continued. From this comparison, it can be concluded that the proposed method can find a true optimal solution from baseline experiment data.

The FE-analysis-based optimization results using the ideal plate model deviate from those of the proposed method, whereas the results from FEM with an adjusted plate model are fairly close to them. The optimization results is Figures 13(c) and 13(d) shows that the distribution of beam widths is sensitive to the boundary condition of the baseline plate. To get correct optimization results, extra model adjustment procedure for the unknown spring support is necessary in the FE modelling procedure in this problem. However, since the proposed method is based on the experimental data containing the effect of the imperfect boundary condition,

TABLE 4

Comparison of the used structural optimization methods

	Proposed method	Perturbation method	FEM optimization
Optimization results	Accurate	Inaccurate for large modal changes	Accurate
Model uncertainty	Considered	Considered	Model adjustment process is required
Measurement load/ computing effort	Measurement load is high for the system having a large number of connecting points	Light	Computing effort is high for the system having a large number of nodal points

the model tuning procedure is not necessary. The unknown spring can be left to an unknown value in the proposed optimization method. This point shows an advantage of the proposed experimental optimization method when it is applied to complex real structures which normally require expensive numerical modelling and verification process.

In spite of the advantages of the proposed method mentioned above, extra efforts are needed for the measurements of FRFs to construct the full FRF matrix of baselines structure. The required number of measurements is $n(n + 1)/2$ for constructing the full FRF matrix of order n [20], whereas n measurements are needed in the modal domain methods to obtain only one column or row of FRF matrix. The measurement load becomes heavy when a structure has a large number of connecting degrees of freedom. Also it is obvious that the optimization results are valid when the measurement of FRF is sufficiently accurate. Table 4 summarizes the merits and demerits of each modification method.

6. CONCLUSIONS

A test-data-based structural optimization procedure to raise eigenvalues has been presented. The modified system is modelled by using a substructure-coupling concept to obtain a considerable improvement in the natural frequency. The system matrix consists of summations of measured FRFs at interface co-ordinates. Proportional design variables were considered to treat the actual structure changes. Consequently, a system equation and an eigenvalue sensitivity equation for successive modifications can be easily formulated using the measured baseline FRFs without any numerical model.

The proposed method was applied to an optimization of beam stiffeners. The beam modifications is modelled by the combination of frequency response elements. Optimal widths of distributed beam stiffeners were calculated to obtain 32% improvement in the fundamental natural frequency of the combined system.

The performance of the optimization results was compared with those obtained by the linearized modal perturbation method and the FEM-based optimization method. The comparisons indicate that the proposed method can find true optimized structural change since the non-linear nature of the natural frequency variation can be predicted from baseline experimental data even when some of the structural parameters are uncertain.

REFERENCES

1. H. M. ADELMAN 1992 *Structural Optimization* **5**, 3–11. Experimental validation of the utility of structural optimization.
2. Y. M. RAM, S. G. BRAUN and J. BLECH 1988 *Journal of Sound and Vibration* **125**, 203–209. Structural modifications in truncated systems by the Rayleigh–Ritz method.
3. Y. M. LUK and L. D. MITCHELL 1984 *Proceedings of the* 2nd *International Modal Analysis Conference*, 930-936. Implementation of dual modal space structural modification method.
4. B. P. WANG 1987 *The International Journal of Analytical and Experimental Modal Analysis* **2**, 50–58. Structural dynamic optimization using reanalysis technique.
5. W. WANG, Q. ZHANG, R. J. ALLEMANG and D. L. BROWN 1990 *Proceedings of the* 8th *International Modal Analysis Conference*, 946–953. Optimization of structural redesign with dynamic constraints.
6. P. VANHONACKER 1982 *Proceedings of the* 1st *International Modal Analysis Conference*, 534–541. Sensitivity analysis of mechanical structures based on experimentally determined modal parameters.
7. J. F. BALDWIN and S. G. HUTTON 1985 *American Institute of Aeronautics and Astronautics Journal* **23**, 1737–1743. Natural modes of modified structure.
8. P. AVITABILE and J. C. O'CALLAHAN 1991 *The International Journal of Analytical and Experimental Modal Analysis* **6**, 215–235. Understanding structural dynamic modification and the effects of truncation.
9. B. P. WANG 1985 *Proceedings of the* 3rd *International Modal Analysis Conference*, 53–58. The limitation of local structural dynamic modification.
10. K. B. ELLIOTT and L. D. MITCHELL 1985 *Proceedings of the* 3rd *International Modal Analysis Conference*, 471–476. Realistic structural modifications: Part I. Theoretical development.
11. K. -J. CHANG and Y. -P. PARK 1998 *Mechanical Systems and Signal Processing* **12**, 525–541. Substructural dynamic modification using component receptance sensitivity.
12. A. SIMPSON 1980 *Aeronautical Journal* **84**, 417–433. The Kron's methodology and practical algorithms for eigenvalue, sensitivity and response analysis of large scale structural systems.
13. K. -M. WON and Y. -S. PARK 1998 *Journal of Sound and Vibration* **213**, 801–812. Optimal support positions for a structure to maximize its fundamental natural frequency.
14. J. -Y. LIAO and C. -C. TSE 1993 *Mechanical Systems and Signal Processing* **7**, 89–104. An algebraic approach for the modal analysis synthesized substructure.
15. E. K. YEE and Y. G. TSUEI 1989 *American Institute of Aeronautics and Astronautics Journal* **27**, 1083–1088. Direct component modal synthesis technique for system dynamic analysis.
16. E. K. YEE and Y. G. TSUEI 1991 *American Institute of Aeronautics and Astronautics Journal* **27**, 1973–1977. Methods for shifting natural frequencies of damped mechanical systems.
17. C. -H. CHU and M. W. TRETHEWEY 1998 *Journal of Sound and Vibration* **211**, 335–353. Rapid structural design change evaluation with and experiment based FEM.

18. M. Mitchell and G. C. Pardoen 1988 *Proceedings of the 6th International Modal Analysis Conference*, 566–571. The estimation of rotational degree-of-freedom using shape function.

19. M. S. Bazara, H. D. Sherali and C. M. Shetty 1993 *Nonlinear Programming*: *Theory and Algorithms*, 448–451. Singapore: John Wiley and Sons, Inc., second edition.

20. D. J. Ewins 1984 *Modal Testing*: *Theory and Practice*, 204–207. England: Research Studies Press Ltd., first edition.